CrossMark

# Thermal decomposition of fire-retarded wood flour/polypropylene composites

## Kinetic property and degradation mechanisms

Lichao Sun[1,2] · Qinglin Wu[2] · Yanjun Xie[1] · Kunlin Song[2] · Sunyoung Lee[3] · Qingwen Wang[1]

**Abstract** The influence of magnesium hydroxide (MH), expandable graphite (EG), and ammonium polyphosphate (APP) on the kinetic property and degradation mechanisms of wood flour/polypropylene composites (WPPC) was investigated using thermogravimetric (TG) analysis. The kinetic parameters were determined using Kissinger and Flynn–Wall–Ozawa (F–W–O) methods. Criado method was used to investigate the probable degradation mechanisms. Thermogravimetric results indicated that EG and APP accelerated the degradation process of wood flour and promoted an increase in the conversion value at low temperatures. The activation energy values obtained through Kissinger and F–W–O methods were 161–178 kJ mol$^{-1}$ (wood flour degradation stage) and 234–305 kJ mol$^{-1}$ (polypropylene degradation stage) for WPPC with or without fire retardants. The degradation mechanism of wood flour occurred by diffusion in three-dimensional processes when the conversion value was below 0.8. Polypropylene and fire retardants had no direct influence on the degradation mechanism of wood flour. In the polypropylene decomposition stage, the degradation of WPPC without fire retardant followed phase-boundary-controlled reaction mechanism. However, the behavior of WPPC incorporation of MH, EG, or APP was governed by nucleation and growth mechanism.

**Keywords** WPC · Fire retardants · TG · Activation energy · Kinetic property · Degradation mechanisms

## Introduction

As a green, environmentally friendly, and renewable bio-composite [1], wood–plastic composites (WPCs) were gaining market share in residential construction applications on decking, roof tiles, siding, window, and door profiles [2, 3]. However, WPCs show an increased fire risk in comparison with wood because of the high heating value of polyolefin polymers [4]. To reduce the flammability of WPCs, many methods were used to treat the WPCs, and the most expeditious method used to acquire flame retardancy was the incorporation of fire retardants during the compounding process [5–12].

Various methods have been developed for evaluating the effectiveness of fire retardant treated WPCs, including thermal analysis, tunnel flame-spread tests, critical oxygen index tests, smoke production tests, fire tube test, cone calorimeter, and analysis of solid residue or gaseous products of thermal decomposition [13–17]. Among these methods, TG analysis was a simple, convenient, and fast method for evaluating the pyrolysis under air or inert gas flow [18]. Numerous investigations were implemented in order to determine the degradation kinetics and mechanisms of natural fibers and plastic, respectively. Yao et al. [19] obtained the apparent activation energy of 160–170 kJ mol$^{-1}$ for ten types of natural fibers using TG

✉ Qinglin Wu
  qwu@agcenter.lsu.edu

✉ Qingwen Wang
  qwwang@nefu.edu.cn

1   Key Laboratory of Bio-based Material Science and Technology (Ministry of Education), Northeast Forestry University, Harbin 150040, Heilongjiang, China

2   School of Renewable Natural Resources, Louisiana State University Agricultural Center, Baton Rouge, LA 70803, USA

3   Department of Forest Products, Korea Forest Research Institute, Seoul 130-712, Korea

Springer

**Table 1** Sample formulations of WPPC

| Sample | WF/% | PP/% | Lubricant/% | MH/% | EG/% | APP/% | MAPP/% |
|--------|------|------|-------------|------|------|-------|--------|
| CTC | 60 | 33 | 5 | 0 | 0 | 0 | 2 |
| MHC | 40 | 33 | 5 | 20 | 0 | 0 | 2 |
| EGC | 40 | 33 | 5 | 0 | 20 | 0 | 2 |
| APPC | 40 | 33 | 5 | 0 | 0 | 20 | 2 |

*WF* wood flour, *PP* neat polypropylene, *MH* magnesium hydroxide, *EG* expandable graphite, *APP* ammonium polyphosphate, *MAPP* maleic anhydride-grafted polypropylene

analysis. Gronli et al. [20] compared the thermogravimetric curves of several hardwoods and softwoods. A comparison between both types of wood showed that the decomposition of softwood started at lower temperatures and that the hemicellulose and cellulose zone were wider. Kumar et al. [21] investigated the thermal decomposition of cornstalks by TG in nitrogen and air atmospheres. The results showed that: Kinetic parameters were similar only at slow heating rates, the second stage occurred very rapidly, and activation energy in air was higher than in nitrogen atmosphere at higher heating rates. Poletto et al. [22] found that the woods' (*Pinus elliottii*, *Eucalyptus grandis*, *Mezilaurus itauba*, and *Dipteryx odorata*) degradation mechanism occurred by diffusion processes when the conversion value was below 0.4. When the conversion value was above 0.5, the degradation mechanism was a result of random nucleation with one nucleus in each particle. The activation energy was calculated by Aboulkas et al. [23] through the iso-conversional methods (Friedman, Kissinger, Flynn–Wall–Ozawa) without pre-assumption regarding the conversion model fulfilled by the reaction. The activation energy values obtained were 179–188 kJ mol$^{-1}$ for PP, and the pyrolysis reaction models of PP was accounted by "contracting cylinder" model.

In recent years, most of the literature on fire-retarded WPPC was used to determine the mass loss and identify the decomposition of material at a certain temperature using a thermogravimetric analyzer. However, few investigations were made on kinetic property and degradation mechanisms. Therefore, it is essential to obtain an in-depth knowledge on pyrolysis of WPPC with or without fire retardants in order to gain further understanding of the combustion and gasification processes. In this paper, magnesium hydroxide (MH), expandable graphite (EG), and ammonium polyphosphate (APP) were selected to study on the WPCs, because they are widely used as fire retardant in polymer and its composites field. The objective of present study was to determine the kinetic parameters and degradation mechanisms of WPPC incorporated with MH, EG, and APP using the TG methodology.

## Experimental

### Materials

Wood flour (WF) with 20-mesh particle size was supplied by American Wood Fiber Inc. (Schofield, WI, USA). Neat polypropylene copolymer (PP) (H00C-00) with a melt flow index of 0.7 g 10 min$^{-1}$ at 230 °C/2.16 kg was purchased from Ineos Olefins & Polymer Co. (League City, TX, USA). Maleic anhydride-grafted polypropylene (MAPP) pellet (Eastman$^{TM}$ G-3003) was provided by Eastman Chemical Products Co. (Kingsport, TN, USA), and used as compatibilizer for immiscible WF and PP blends. Lubricant powder (TPW 306) was supplied by Struktol Co. (Stow, OH, USA), and was used to improve the processing performance of the products. MH (MAGNIFIN H-5), EG (220-80N), and APP powders (200503) were provided by Albemarle Co. (Baton rouge, LA, USA), Graftech International Holding Inc. (Lakewood, OH, USA), and JLS Flame Retardants Chemical Co. Ltd. (Hangzhou, Zhejiang, China), respectively. Moreover, the structure of EG is lamellar, and crystalIIstructure for the APP.

**Table 2** Kinetic methods used in evaluating activation energy in this study

| Methods | Expressions | Plots |
|---------|-------------|-------|
| Kissinger | $\ln\left(\beta/T_p^2\right) = \ln(AR/E_\alpha) + (1/T_p)(-E_\alpha/R)$ | $\ln\left(\beta/T_p^2\right)$ against $1/T_p$ |
| Flynn–Wall–Ozawa | $\log\beta = \log[AE_\alpha/Rg(\alpha)] - 2.315 - 0.4567E_\alpha/RT$ | $\log\beta$ against $1/T$ |
| Criado | $Z(\alpha)/Z(0.5) = g(\alpha)f(\alpha)/g(0.5)f(0.5) = (T_\alpha/T_{0.5})^2(d\alpha/dt)_\alpha/(d\alpha/dt)_{0.5}$ | $Z(\alpha)/Z(0.5)$ against $\alpha$ |

**Table 3** Expressions of $f(\alpha)$ for the most frequently used mechanisms of degradation processes

| Mechanisms | $g(\alpha)$ | $f(\alpha)$ |
| --- | --- | --- |
| Nucleation and growth (Avrami equation 1)-A2 | $[-\ln(1-\alpha)]^{1/2}$ | $2(1-\alpha)[-\ln(1-\alpha)]^{1/2}$ |
| Nucleation and growth (Avrami equation 2)-A3 | $[-\ln(1-\alpha)]^{1/3}$ | $3(1-\alpha)[-\ln(1-\alpha)]^{2/3}$ |
| Nucleation and growth (Avrami equation 3)-A4 | $[-\ln(1-\alpha)]^{1/4}$ | $4(1-\alpha)[-\ln(1-\alpha)]^{3/4}$ |
| Phase-boundary-controlled reaction (motion in one dimension)-R1 | $\alpha$ | $1$ |
| Phase-boundary-controlled reaction (contracting area)-R2 | $1-(1-\alpha)^{1/2}$ | $2(1-\alpha)^{1/2}$ |
| Phase-boundary-controlled reaction (contracting volume)-R3 | $1-(1-\alpha)^{1/3}$ | $3(1-\alpha)^{2/3}$ |
| Diffusion in one dimension-D1 | $\alpha^2$ | $\alpha/2$ |
| Diffusion in two dimensions (Valensi equation)-D2 | $(1-\alpha)\ln(1-\alpha)+\alpha$ | $[-\ln(1-\alpha)]^{-1}$ |
| Diffusion in three dimensions (Jander equation)-D3 | $[1-(1-\alpha)^{1/3}]^2$ | $3(1-\alpha)^{2/3}/[2(1-(1-\alpha)^{1/3})]$ |
| Diffusion in three dimensions (Ginstling–Brounshtein equation)-D4 | $(1-2\alpha/3)-(1-\alpha)^{2/3}$ | $3/2[(1-\alpha)^{1/3}-1]$ |
| Random nucleation with one nucleus of individual particle-F1 | $-\ln(1-\alpha)$ | $(1-\alpha)$ |
| Random nucleation with two nuclei of individual particles-F2 | $1/(1-\alpha)$ | $(1-\alpha)^2$ |
| Random nucleation with three nuclei of individual particles-F3 | $1/(1-\alpha)^2$ | $(1-\alpha)^3/2$ |

## Sample preparation

Table 1 lists the sample formulations for WPPC. A total of four types of composites were prepared, including WPPC as control (CTC), WPPC with MH (MHC), WPPC with EG (EGC), and WPPC with APP (APPC). WF was dried in a convection oven at 105 °C for 24 h before used. A Leistritz Micro-27 corotating parallel twin-screw extruder (Leistritz Corporation, Allendale, NJ) was used to manufacture the composites. The Leistritz machine was equipped with two mass-in-loss feeders, and was controlled by an independent computer with commercial software. Manufacturing temperatures in the main processing zones were controlled between 170 and 180 °C, applying an extruder rotation speed of 55 rpm.



**Fig. 1** TG and DTG curves of PP, PP/MAPP/lubricant, and CTC at a heating rate of 10 °C min$^{-1}$

## Thermal analysis

Thermogravimetric (TG) analysis was performed on a TA Instrument TGA Q50 from 30 to 600 °C at four different heating rates of 5, 10, 15, and 20 °C min$^{-1}$. A high purity nitrogen stream (99.5 % nitrogen, 0.5 % oxygen content) was continuously passed into the furnace at a flow rate of 40 mL min$^{-1}$ at room temperature and atmospheric pressure. Before starting each run, nitrogen was used to purge the furnace for 60 min to establish an inert environment in order to prevent any unwanted oxidative decomposition. Approximately 5 mg of each sample was used. The results obtained from TG were used to calculate the kinetic parameters.
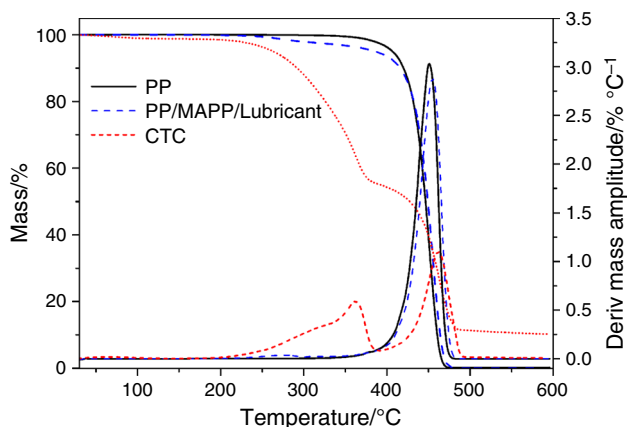
## Theoretical approach

The fundamental equation used in all kinetic studies is generally described as [24]:

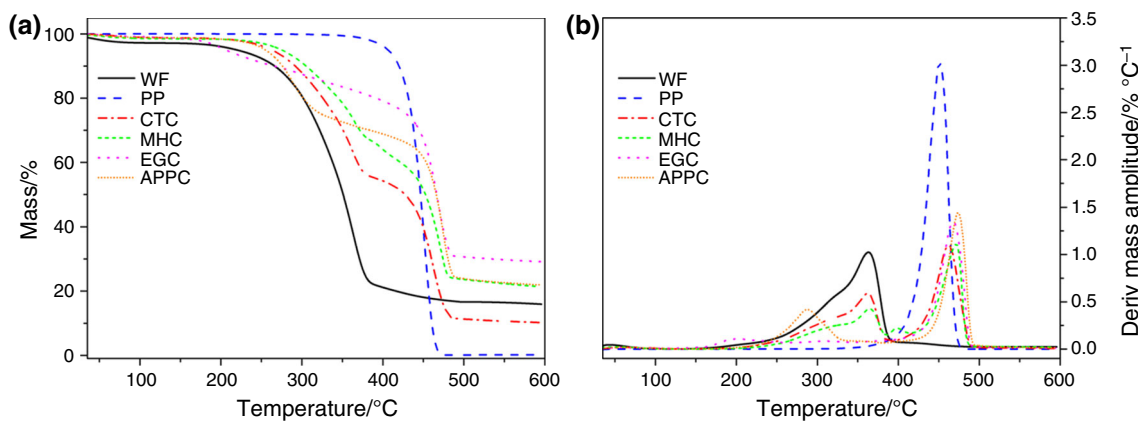$$\mathrm{d}\alpha/\mathrm{d}t = kf(\alpha) \tag{1}$$

where $k$ is the rate constant and $f(\alpha)$ is the reaction model, a function dependent on the reaction mechanism. Equation 1 expresses the rate of conversion, $\mathrm{d}\alpha/\mathrm{d}t$, at a constant temperature as a function of the rate constant and the reduction in the reactant concentration. In this study, the conversion $\alpha$ is defined as:

$$\alpha = (m_\mathrm{o} - m_\mathrm{t})/(m_\mathrm{o} - m_\mathrm{f}) \tag{2}$$
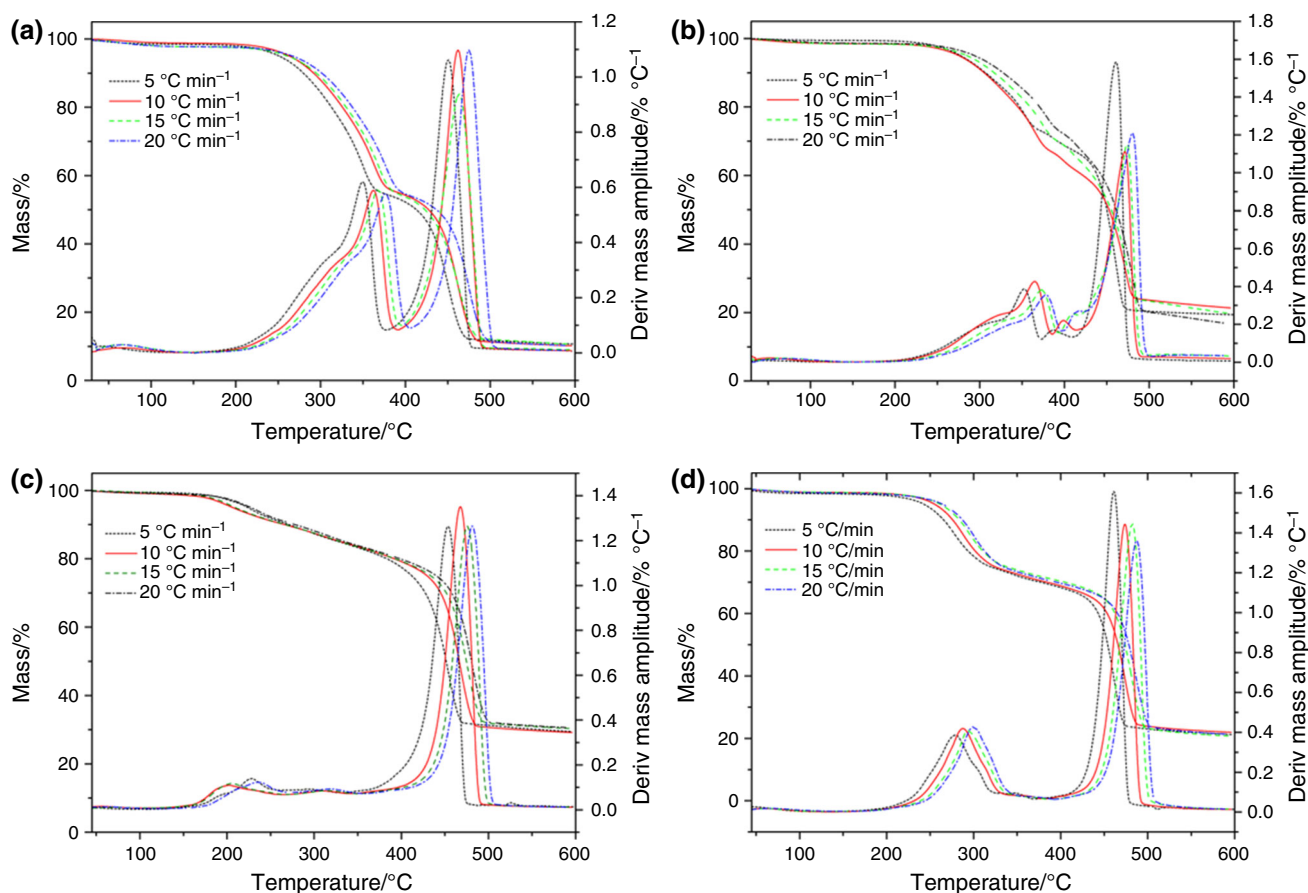
where $m_\mathrm{o}$ is the initial mass of the sample, $m_\mathrm{f}$ is the final mass, and $m_\mathrm{t}$ is the sample's mass at time ($t$). The rate constant $k$ is generally given by the Arrhenius equation [25]:

Fig. 2 TG (**a**) and DTG (**b**) curves of samples at a heating rate of 10 °C min$^{-1}$



Fig. 3 TG and DTG curves of the samples at different heating rates: **a** CTC, **b** MHC, **c** EGC, and **d** APPC

$$k = A \exp(-E_\alpha/RT) \qquad (3)$$

where $A$ is the frequency factor, $E_\alpha$ is the apparent activation energy (kJ mol$^{-1}$), $R$ is gas constant (8.314 J mol$^{-1}$ K$^{-1}$), and $T$ is the absolute temperature (K). The combination of Eqs. (1) and (3) gives the following relationship:

$$d\alpha/dt = Af(\alpha)\exp(-E_\alpha/RT) \qquad (4)$$

for a dynamic TG analysis in non-isothermal conditions with a linear heating rate of $\beta = dT/dt$; Eq. (3) can be written as:

$$d\alpha/dT = (A/\beta)f(\alpha)\exp(-E_\alpha/RT) \qquad (5)$$
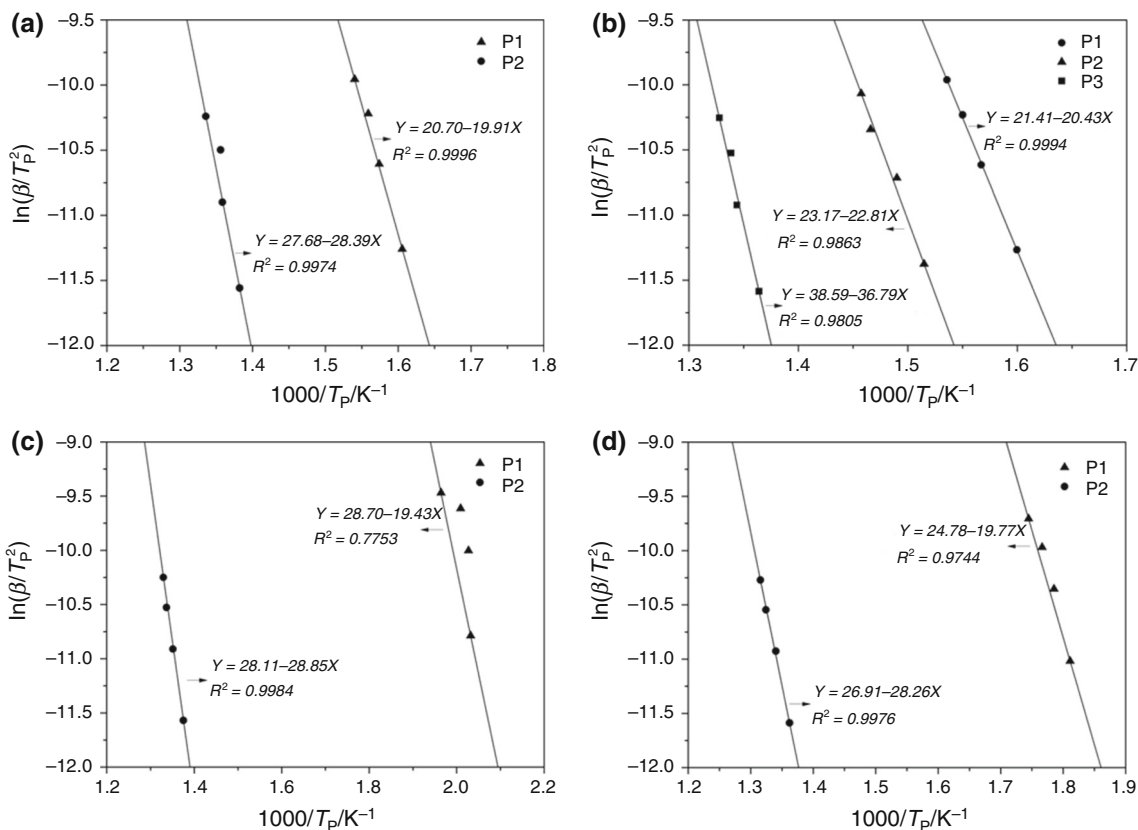
Fig. 4 Linear plots of $\ln\left(\beta/T_{\mathrm{P}}^2\right)$ versus $1/T_{\mathrm{p}}$ for samples in Kissinger methods: **a** CTC, **b** MHC, **c** EGC, and **d** APPC

**Table 4** Apparent activation energy of samples calculated by Kissinger and F–W–O methods

| Samples | Kissinger | | Flynn–Wall–Ozawa | |
|---|---|---|---|---|
| | $E_\alpha$/kJ mol$^{-1}$ | R | $E_\alpha$/kJ mol$^{-1}$ | R |
| WF | 169 | 0.9998 | [c]176[d] (3.3) | 0.9909 (0.009) |
| PP | 231 | 0.9998 | 240 (4.7) | 0.9932 (0.003) |
| CTC[a] | 165 | 0.9998 | 168 (6.2) | 0.9898 (0.009) |
| CTC[b] | 236 | 0.9987 | 251 (19.0) | 0.9907 (0.006) |
| MHC[a] | 170 | 0.9997 | 173 (5.6) | 0.9903 (0.005) |
| MHC[b] | 305 | 0.9902 | 296 (11.0) | 0.9936 (0.002) |
| EGC[a] | 161 | 0.8805 | 178 (4.6) | 0.9836 (0.004) |
| EGC[b] | 240 | 0.9992 | 261 (6.8) | 0.9933 (0.002) |
| APPC[a] | 164 | 0.9871 | 168 (4.5) | 0.9975 (0.002) |
| APPC[b] | 234 | 0.9988 | 242 (6.9) | 0.9923 (0.002) |

[a] Main decomposition of wood flour

[b] Main decomposition of PP

[c] The constant value was the average value of the activation energy at the decomposition stage of WF or PP

[d] The standard deviation

Equations (4) and (5) are the fundamental expressions of analytical methods to calculate kinetic parameters on the basis of TG data.

The degradation kinetic analyses were performed using the following three methods, which are summarized in Table 2. In the Kissinger method, $\ln(\beta/T_{\mathrm{p}}^2)$ is plotted against $(1/T_{\mathrm{p}})$ for a series of experiments at different heating rates with peak temperature, and the $E_\alpha$ can be calculated from the slope of the line. $T_{\mathrm{p}}$ is the peak temperature obtained from the differential thermogravimetric analysis (DTG) curves. The iso-conversional Flynn–Wall–Ozawa (F–W–O) method is the integral method, which leads to $-E_\alpha/R$ from the slope of the line determined by plotting $\log\beta$ against $1/T$ at any certain conversion.

The degradation reaction mechanism can be determined using the Criado method [26]; the master curves as a function of the conversion degree corresponding to the different models listed in Table 3 were obtained according to Eq. (6):

$$Z(\alpha) = g(\alpha)f(\alpha) \tag{6}$$

The standard Eq. (5) can be shown as follows:
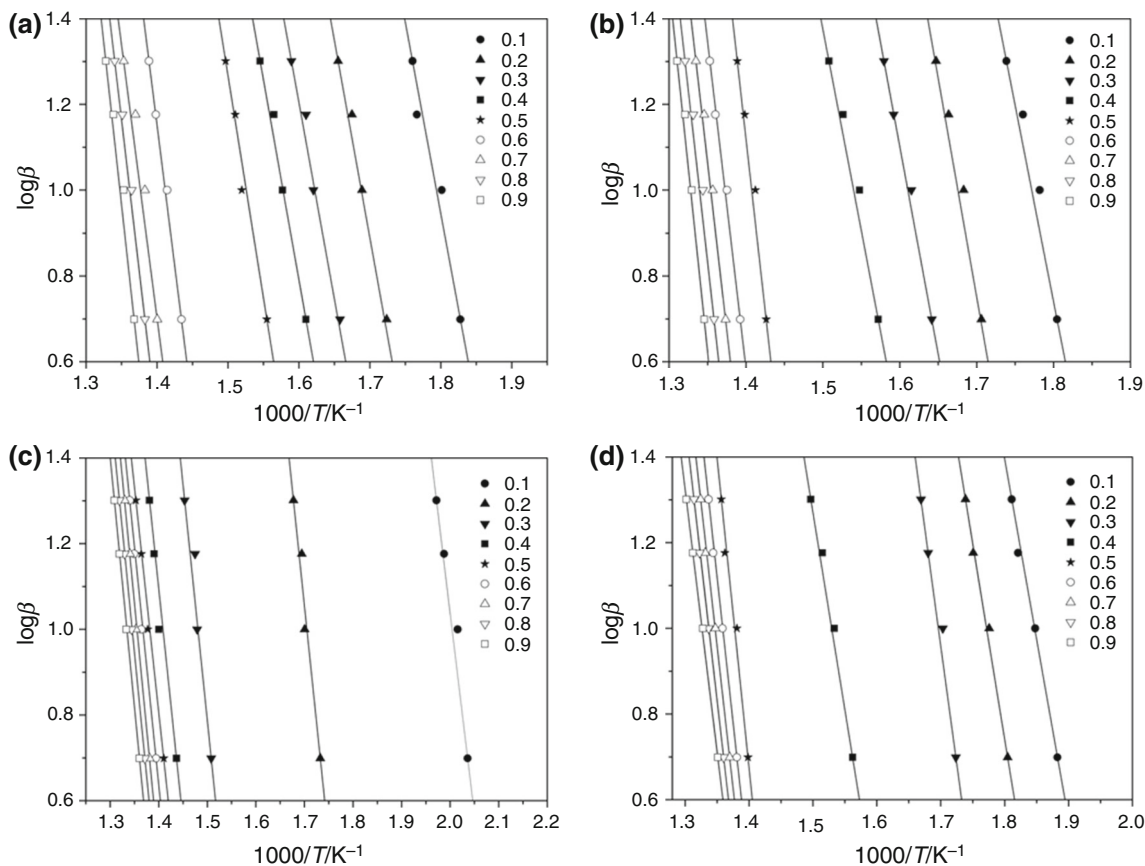
**Fig. 5** Linear plots of $\log\beta$ versus $1/T$ for samples in F–W–O methods: **a** CTC, **b** MHC, **c** EGC, and **d** APPC

$$d\alpha/f(\alpha) = (A/\beta)\exp(-E_\alpha/RT)dT \qquad (7)$$

which is integrated with the initial condition of $\alpha = 0$ at $T = T_0$ to obtain the following expression:

$$g(\alpha) = \int_0^\alpha d\alpha/f(\alpha) = (A/\beta) \int_{T_0}^T \exp(-E_\alpha/RT)dT \qquad (8)$$

Using an asymptotic approximation for the resolution of Eq. (8) ($2RT/E \ll 1$), the following equation can be obtained:

$$\ln\left[g(\alpha)/T^2\right] = \ln(AR/\beta E_\alpha) - E_\alpha/RT \qquad (9)$$

Combining Eq. (4) with Eq. (9), the following equation is obtained:

$$\begin{aligned} Z(\alpha)/Z(0.5) &= g(\alpha)f(\alpha)/g(0.5)f(0.5) \\ &= (T_\alpha/T_{0.5})^2 (d\alpha/dt)_\alpha/(d\alpha/dt)_{0.5} \end{aligned} \qquad (10)$$

where 0.5 refers to the conversion in $\alpha = 0.5$. The left side of Eq. (10) is a reduced theoretical curve, which is characteristic of each reaction mechanism, whereas the right side of the equation associated with the reduced rate can be obtained from experimental data. By comparing these two curves, the type of mechanism involved in the thermal degradation can be identified.

# Results and discussion

## Thermal degradation analysis

Figure 1 shows that the onset decomposition temperature of the mixtures of PP, MAPP, and lubricant was lower than pure PP, because of the decomposition of MAPP and lubricant. However, the decomposition process of pure PP did not change significantly due to the too little MAPP and lubricant in proportion of the sample. Therefore, the influence of MAPP and lubricant on PP decomposition can be ignored compared with wood flour. Figure 2a shows that WF and PP had its own distinctive temperature ranges for the degradation processes, and a distinct thermal decomposition peak appeared at 364 and 450 °C for WF and PP (Fig. 2b), respectively. However, CTC had two main thermal decomposition peaks resulted mainly from the thermal decomposition of WF and PP, and the second decomposition peak shifted to a higher temperature, which indicated that the thermal protective carbonaceous layer produced from the degradation of wood flour can enhance the thermal stability of the PP. It was observed with a weak peak at 398 °C for MHC, which was normally considered as the result of thermal decomposition of MH [13]. At the
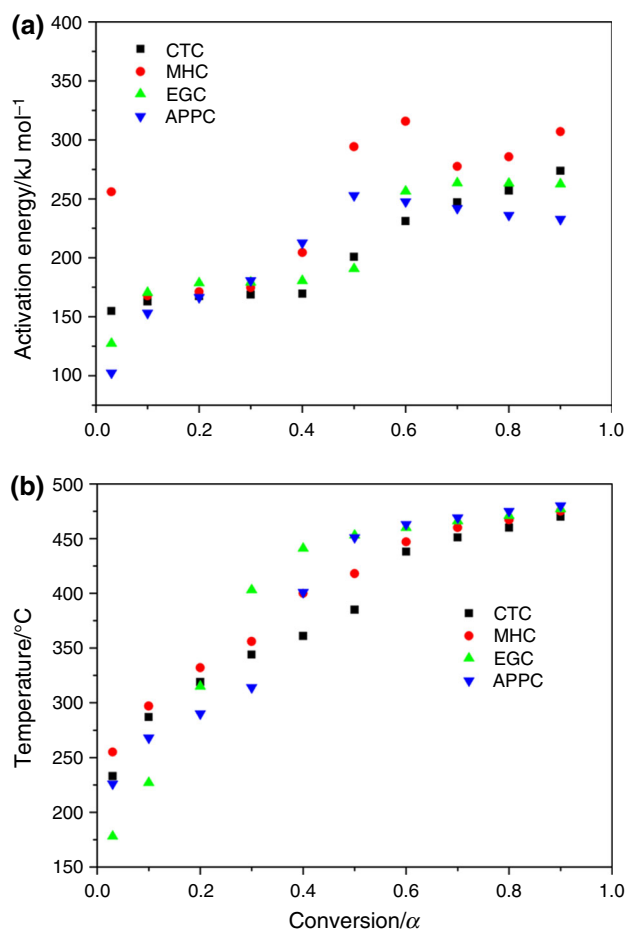
**Fig. 6** **a** Activation energy as a function of conversion using F–W–O method. **b** Temperature as a function of conversion at a heating rate of $10\ °C\ min^{-1}$

first thermal decomposition stage, EGC began the degradation process at lower temperature than CTC, which can be deduced that acidic EG promoted thermal degradation of wood flour and mass loss at lower temperatures [27]. However, the decomposition rate of EGC was lower compared with CTC, which indicated that EG slowed the thermal decomposition of the WF in EGC system. The first decomposition peak in APPC system narrowed down and shifted to lower temperature, which showed that APP promoted the thermal degradation of WF in WPPC system earlier and char formation. At the thermal decomposition stage of PP, all the decomposition peaks with fire retardants shifted to higher temperature and the residue significantly increased. Figure 3 shows a lateral shift to higher temperatures for the decomposition peaks as the heating rate increased. The rate of mass loss also reflected that the lateral shift with an increase in the heating rate was increased from 5 to $20\ °C\ min^{-1}$. The displacement of TG curves with heating rate was described in the literature by different researchers [28, 29].

## Calculation of the activation energy

The results obtained from TG were elaborated according to model-free methods to calculate the kinetic parameters. The activation energy ($E_\alpha$) values were calculated from Kissinger equation (Table 2), and the peak temperatures were obtained from Fig. 3. The Kissinger plots for the samples are shown in Fig. 4, and the regression equations and the square of the correlation coefficient ($R$) are also presented. Table 4 lists the values of $E_\alpha$, which were derived from the slope. Figure 5 shows the results of application of F–W–O method with $\alpha$ values from 0.1 to 0.9. F–W–O equation (Table 2) was used, and the $E_\alpha$ values of samples were obtained from plot of $\log\beta$ against $1/T$ at a fixed conversion value with the slope of such a line being $0.4567\ E_\alpha/RT$.

As shown in Fig. 6a, b, at the beginning of decomposition ($\alpha = 0.03$), the temperature of CTC, MHC, EGC, and APPC were 227, 252, 175, and 225 °C, and the $E_\alpha$ values were 154, 255, 127, and 102 kJ mol$^{-1}$, respectively. These results confirmed that the EG and APP promoted the degradation of wood flour at relatively low temperatures, and reduced the thermal stability of wood flour. However, the value of 255 kJ mol$^{-1}$ for MHC is probably a technical artifact, because it is much higher than the value at the wood decomposition stage and no reference refers to these results. As the thermal decomposition proceeding, the $E_\alpha$ values of CTC almost remained constant until $\alpha = 0.4$, while $\alpha = 0.3$ and 0.5 for MHC and EGC. However, the $E_\alpha$ values of APPC increased with the increasing of conversion below 0.5. This indicated that APP improved the thermal stability of wood flour with the thermal decomposition proceeding. When conversion value was between 0.5 and 0.9, mainly the degradation of PP occurred. The samples showed a different thermal degradation behavior compared with low conversion value. Once again, MHC had the highest $E_\alpha$ values at the same conversion value (Fig. 6a). In this range of conversion, the degradation process in PP was probably influenced by the degradation of fire retardants and the char content. These factors led to an acceleration or deceleration of the degradation of PP.

Table 4 summarizes the $E_\alpha$ values for all of samples studied. It was clearly observed that the $E_\alpha$ values of CTC, MHC, EGC, and APPC samples calculated using the two methods followed the same trend at PP decomposition stage, in the order MHC > EGC > CTC > APPC, even if there were differences between the $E_\alpha$ values obtained by the Kissinger and F–W–O methods. However, it followed the order EGC > MHC > CTC ≈ APPC at wood flour decomposition stage, except for the $E_\alpha$ value of EGC obtained by the Kissinger. The first decomposition peak was caused by catalysis of the acidic EG, where only a small amount of cellulose decomposed in this step.
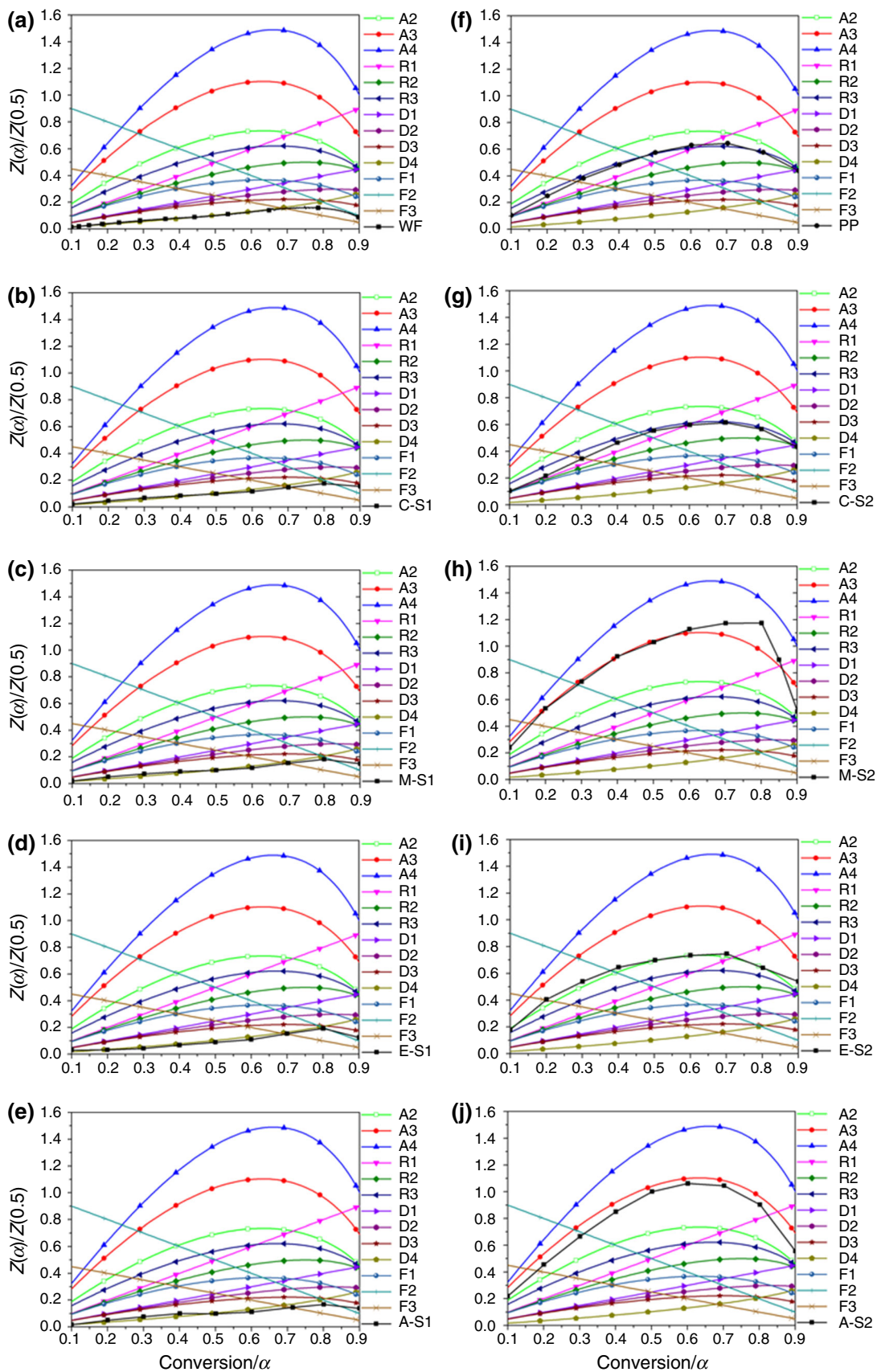
◀**Fig. 7** Master curves and experimental data obtained using the Criado method: **a** WF, **b** CTC-stage1, **c** MHC-stage1, **d** EGC-stage1, **e** APPC-stage1, **f** PP, **g** CTC-stage2, **h** MHC-stage2, **i** EC-stage2, and **j** APPC-stage2

## Discussion on the degradation mechanisms

The $Z(\alpha)/Z(0.5)$ master curves can be plotted using Eq. (6) according to different reaction mechanisms $g(\alpha)$ shown in Table 3. The used experimental TG data were from TG curve at 10 °C min$^{-1}$ heating rates, and the two thermal degradation stages were calculated separately. Figure 7 shows the $Z(\alpha)/Z(0.5)$ master and experimental curves of WF, PP, CTC, MHC, EGC, and APPC, respectively. The experimental curve of WF nearly overlapped the D4 curve in the range of $\alpha = 0.1–0.8$ (Fig. 7a), which referred to a diffusion process in three dimensions. Similar results were described by other researchers for other cellulosic fibers [22, 24, 30]. Figure 7b–e shows the same curves ($\alpha = 0.1–0.7$) for WPPC with or without fire retardants comparing with WF, which indicated that PP and fire retardants had no direct influence on the degradation mechanism of WF. When the conversion value was higher than 0.8, it was difficult to fit the experimental curves to the master curves due to the decomposition of PP or fire retardants. Figure 7f, g exhibits that the experimental curves of PP and CTC almost overlapped the R3 curves, which corresponded to phase-boundary-controlled reaction (contracting volume). However, the shape of the experimental curves for MHC ($\alpha = 0.1–0.6$) and APPC were similar to A3 curve (Fig. 7h, j), and matched to A2 curve for EGC (Fig. 7i).

## Conclusions

The kinetic property of WF, PP, and WPPC with or without fire retardants was accurately determined from a series of experiments at four heating rates. The activation energy was calculated by the Kissinger and F–W–O methods without pre-assumption regarding the conversion model fulfilled by the reaction. A general activation energy value range of 161–178 kJ mol$^{-1}$ at WF degradation stage and 234–305 kJ mol$^{-1}$ at PP degradation stage were obtained for WPPC with and without fire retardants. Criado method was successfully utilized to predict the degradation mechanisms of WF, PP, and WPPC. The degradation mechanism of WF followed diffusion in three-dimensional process mechanism (model D3) when the conversion value was below 0.8. In the wood flour decomposition stage, the degradation mechanisms of WPPC incorporation with fire retardants were not significantly changed. PP and CTC were corresponded to phase-boundary-controlled reaction

(model R3). However, the degradation mechanisms of WPPC incorporation of fire retardants were significantly changed at the PP decomposition stage. MHC and APPC followed nucleation and growth mechanisms (model A2), whereas EGC can be described by nucleation and growth mechanism (model A1).

## References

1. La Mantia FP, Morreale M. Green composites: a brief review. Compos Part A Appl Sci Manuf. 2011;42:579–88.
2. Hazarika A, Maji TK. Thermal decomposition kinetics, flammability, and mechanical property study of wood polymer nanocomposite. J Therm Anal Calorim. 2014;115:1679–91.
3. Li B, He J. Investigation the mechanical property, flame retardancy and thermal degradation of LLDPE–wood fiber composites. Polym Degrad Stab. 2004;83:241–6.
4. Pearce EM, Khanna YP, Reucher D. Thermal characterization of polymeric materials. New York: Academic Press; 1981.
5. Ayrilmis N, Akebulut T, Dundar T, White RH, Mengeloglu F, Buyuksari U, Candan Z, Avci E. Effect of boron and phosphate compounds on physical, mechanical, and fire properties of wood–polypropylene composites. Constr Build Mater. 2012;33:62–9.
6. Sain M, Park SH, Suhara F, Law S. Flame retardant and mechanical properties of natural fiber–PP composites containing magnesium hydroxide. Polym Degrad Stab. 2004;83(2):363–7.
7. Stark NM, White RH, Mueller SA, Osswald TA. Evaluation of various fire retardants for use in wood flour–polyethylene composites. Polym Degrad Stab. 2010;95:1903–10.
8. Naumann A, Seefeldt H, Stephan I, Braun U, Noll M. Material resistance of flame retarded wood–plastic composites against fire and fungal decay. Polym Degrad Stab. 2012;97:1189–96.
9. Yoshihiko A, Sakae N, Yuta T, Kyouhei T, Toshikazu U, Tatsuya T. Improvement on fire retardancy of wood flour/polypropylene composites using various fire retardants. Polym Degrad Stab. 2014;100:79–85.
10. Fang YQ, Wang QW, Guo CG, Song YM, Cooper PA. Effect of zinc borate and wood flour on thermal degradation and fire retardancy of polyvinyl chloride (PVC) composites. J Anal Appl Pyrol. 2013;100:230–6.
11. Azwa ZN, Yousif BF, Manalo AC, Karunasena W. A review on the degradability of polymeric composites based on natural fibres. Mater Des. 2013;47:424–42.
12. Seefeldt H, Braun U, Wagner MH. Residue stabilization in the fire retardancy of wood–plastic composites: combination of ammonium polyphosphate, expandable graphite, and red phosphorus. Macromol Chem Phys. 2012;213:2370–7.
13. Gwon JG, Lee SY, Kim JH. Thermal degradation behavior of polypropylene base wood plastic composites hybridized with metal (aluminum, magnesium) hydroxides. J Appl Polym Sci. 2014;131(7):40120.
14. Bai G, Guo CG, Li LP. Synergistic effect of intumescent flame retardant and expandable graphite on mechanical and flame-retardant properties of wood flour–polypropylene composites. Constr Build Mater. 2014;50:148–53.

15. Nikolaeva M, Karki AT. A review of fire retardant processes and chemistry, with discussion of the case of wood–plastic composites. Baltic For. 2011;17(2):314–26.

16. Seefeldt H, Braun U. A new flame retardant for wood materials tested in wood–plastic composites. Macromol Mater Eng. 2012;297:814–20.

17. Song YM, Wang QW, Gong L, Li CT. Synergistic effects of expandable graphite with ammonium polyphosphate on flame retardancy of wood flour/polypropylene composites. Sci Silvae Sin. 2011;47(7):145–50.

18. Liodakis S, Bakirtzis D, Dimitrakopoulos AP. Autoignition and thermogravimetric analysis of forest species treated with fire retardants. Thermochim Acta. 2003;399:31–42.

19. Yao F, Wu QL, Lei Y, Guo WH, Xu YJ. Thermal decomposition kinetics of natural fibers: activation energy with dynamic thermogravimetric analysis. Polym Degrad Stab. 2008;93:90–8.

20. Gronli MG, Varhegyi G, Blasi CD. Thermogravimetric analysis and devolatilization kinetics of wood. Ind Eng Chem Res. 2002;41:4201–8.

21. Kumar A, Wang LJ, Dzenis YA, Jones DD, Hanna MA. Thermogravimetric characterization of corn stover as gasification and pyrolysis feedstock. Biomass Bioenergy. 2008;32:460–7.

22. Poletto M, Zattera AJ, Santana RMC. Thermal decomposition of wood: kinetics and degradation mechanisms. Bioresour Technol. 2012;126:7–12.

23. Aboulkas A, El Harfi K, El Bouadili A. Thermal degradation behaviors of polyethylene and polypropylene. Part I: pyrolysis kinetics and mechanisms. Energy Convers Manag. 2010;51: 1363–9.

24. Bianchi O, Martins JDN, Fiorio R, Oliveira RVB, Canto LB. Changes in activation energy and kinetic mechanism during EVA crosslinking. Polym Test. 2011;30:616–24.

25. Carrasco F. The evaluation of kinetic-parameters from thermogravimetric data—comparison between established methods and the general analytical equation. Thermochim Acta. 1993; 213:115–34.

26. Criado JM. Kinetic analysis of DTG data from master curves. Termochim Acta. 1978;24:186–9.

27. Wang QW, Li J, Winandy JE. Chemical mechanism of fire retardant of boric acid on wood. Wood Sci Technol. 2004; 38(5):375–89.

28. Yang J, Miranda R, Roy C. Using the DTG curve fitting method to determine the apparent kinetic parameters of thermal decomposition of polymers. Polym Degrad Stab. 2001;73:455–61.

29. Park JW, Oh SC, Lee HP, Kim HT, Yoo KO. A kinetic analysis of thermal degradation of polymers using a dynamic method. Polym Degrad Stab. 2000;67:535–40.

30. Wu Y, Dollimore D. Kinetic studies of thermal degradation of natural cellulosic materials. Thermochim Acta. 1998;324:49–57.